stable terminal C-H bond accompanied by the conversion of the cage geometry to one possessing only triangular faces.

The determination of the structure of **1** renews our interest in the structure of the dianion $[nido\text{-}C_2B_{10}H_{12}]^{2-}$. On the basis of the structure of **1** and those of the metallacarboranes containing the $[C_2B_{10}H_{12}]^{2-}$ ligand, it is anticipated that the structure of the dianion is similar to that of **1**, with the bridge proton removed. Due to the highly fluxional nature of $[nido\text{-}C_2B_{10}H_{12}]^{2-}$, its structure can only be determined with certainty via X-ray diffraction methods. Attempts to accomplish this are in progress.

Acknowledgment. The support of this work by the National Science Foundation (Grant CHE-88-06179) is gratefully acknowledged.

Supplementary Material Available: Listings of crystallographic data (Table I), positional and thermal parameters (Table II), interatomic distances and angles (Table III), distances within the hexagonal faces of the referenced metallacarboranes and **1** (Table A), and distances within the quadrilateral formed by C(7), B(2), B(3), and C(8) of the referenced metallacarboranes and **1** (Table B) (7 pages); a listing of calculated and observed structure factors (Table IV) (13 pages). Ordering information is given on any current masthead page.

(14) Churchill, M. R.; DeBoer, B. G. *Inorg. Chem.* **1974**, *13*, 1411.
(15) Mastryukov, V. S.; Dorofeeva, O. V.; Vilkov, L. V. *Russ. Chem. Rev. (Engl. Transl.)* **1980**, *49*, 1181.

Department of Chemistry and Biochemistry
University of California
Los Angeles, California 90024-1569

Thomas D. Getman
Carolyn B. Knobler
M. Frederick Hawthorne*

Received October 5, 1989

Articles

Contribution from the Department of Chemical and Biological Sciences, Oregon Graduate Center, Beaverton, Oregon 97006-1999

Structure and Water-Oxidizing Capabilities of Dimeric Ruthenium EDTA Complex Ions

Jinzhong Zhou, Wu Xi, and James K. Hurst*

Received April 18, 1989

Low-temperature resonance Raman (RR) spectra of the dimeric $Ru^{III}Ru^{IV}$ ion formed by oxidation of $Ru(edta)OH_2^-$ exhibited a prominent band at 433 cm^{-1}, which shifted to 431 cm^{-1} upon substitution of $[^{18}O]\text{-}H_2O$ in the primary coordination sphere of the precursor ion. A second band, at 324 cm^{-1}, underwent a comparable isotope-dependent shift to lower energies. The RR spectra were insensitive to deuterium substitution. These features establish that the dimer is a μ-oxo ion, i.e., $[Ru(edta)]_2O^{3-}$; from the magnitude of the isotopic shifts, the Ru-O-Ru angle was estimated to be 165°. The reduction potential for the $Ru^{IV}{}_2/Ru^{III}Ru^{IV}$ couple was acid-insensitive over the range pH 2-11, suggesting that the dimer does not contain coordinated H_2O in either oxidation state. Cyclic voltammographic results in neutral solution suggested that $[Ru(edta)]_2O^{2-}$ was unstable with respect to decomposition. A reinvestigation of the water-oxidizing capabilities of this ion by polarographic, gas chromatographic, and mass spectrometric methods failed to reveal O_2 among the gaseous products. Instead, copious quantities of CO_2 were formed, the source of which was coordinated EDTA.

Binuclear ions form upon oxidation of $Ru(edta)(OH_2)^-$ in aqueous solution. Numerous structures have been proposed for the dimers including, in early studies, $L_2Ru^{IV}{}_2$ or mixed-valent $L_2Ru^{III}Ru^{IV}$ ions that are either doubly bridged by dihydroxo, peroxo and hydroxo, superoxo and hydroxo, or aqua and oxo ligands.[1,2] More recently, redox titrations with several oxidants have established that the stable dimeric product is a mixed-valent ion,[3,4] formally $L_2Ru^{III}Ru^{IV}$, although its optical and magnetic properties are indicative of an electronic ground state in which the unpaired spin density is strongly delocalized over both metal centers.[4] Furthermore, the stoichiometry of proton release accompanying oxidation in weakly acidic solutions is consistent only with μ-oxo or dihydroxy ligand bridging.[4] Baar and Anson also proposed conversion to a mixed hydroxo-oxo dibridging system in alkaline solution (pH >10), based upon the titrimetric behavior of the dimer and the pH dependence of the $L_2Ru^{III}Ru^{IV}/L_2Ru^{III}{}_2$ redox couple. They showed that the $L_2Ru^{III}Ru^{IV}$ ion could be further oxidized either chemically with Ce^{4+} or electrochemically to give a spectroscopically distinct species. From a Nernst plot of thin-layer spectroelectrochemical data, they ascertained that one-electron oxidation had occurred, yielding a $L_2Ru^{IV}{}_2$ ion. This latter species was unstable and spontaneously reverted to $L_2Ru^{III}Ru^{IV}$ or a spectroscopically indistinguishable ion. Reduction of the $L_2Ru^{IV}{}_2$ ion was thought to occur at the expense of solvent H_2O, on the basis of the observation of a positive response from a Clark polarographic electrode in the presence of excess Ce^{4+} ion or for solutions poised at a potential that allowed regeneration of the oxidized dimer.[4,5]

Our interest in this ion was prompted by the claim that it could act as a catalyst for water oxidation. Several μ-oxo ruthenium dimers of the type *cis,cis*-$[(bpy)_2Ru(OH_2)]_2O$ have been described that are capable of catalytically oxidizing water electrochemically or in the presence of strong oxidants.[6-9] Although the reaction mechanisms have not yet been identified, salient features are thought to include the presence of coordinated water, which provides access to higher oxidation states via deprotonation,[10] and the μ-oxo bridge, which, by forcing close juxtaposition of hydroxo or oxo ligands in the higher oxidation states, might facilitate reductive elimination of H_2O_2 or O_2.[6,7,9] Additionally, carboxyl

(1) Ezerskaya, N. A.; Solovykh, T. P. *Russ. J. Inorg. Chem. (Engl. Transl.)* **1968**, *13*, 96, and references therein.
(2) Taqui Khan, M. M.; Ramachandraiah, G. *Inorg. Chem.* **1982**, *21*, 2109.
(3) Ikeda, M.; Shimizu, K.; Sato, G. P. *Bull. Chem. Soc. Jpn.* **1982**, *55*, 797.
(4) Baar, R. B.; Anson, F. C. *J. Electroanal. Chem. Interfacial Electrochem.* **1985**, *187*, 265.
(5) Baar, R. B. Ph.D. Dissertation, California Institute of Technology, 1985.
(6) Gilbert, J. A.; Eggleston, D. S.; Murphy, W. A., Jr.; Geselowitz, D. A.; Gersten, S. W.; Hodgson, D. J.; Meyer, T. J. *J. Am. Chem. Soc.* **1985**, *107*, 3855.
(7) Raven, S. J.; Meyer, T. J. *Inorg. Chem.* **1988**, *27*, 4478.
(8) Rotzinger, F. P.; Munavalli, S.; Comte, P.; Hurst, J. K.; Grätzel, M.; Pern, F.-J.; Frank, A. J. *J. Am. Chem. Soc.* **1987**, *109*, 6619.
(9) Nazeeruddin, M. K.; Rotzinger, F. P.; Comte, P.; Grätzel, M. *J. Chem. Soc., Chem. Commun.* **1988**, 872.
(10) Meyer, T. J. *J. Electrochem. Soc.* **1984**, *131*, 221C.

0020-1669/90/1329-0160$02.50/0

group substitution at the 5,5′-positions in the bipyridine ring has been reported to enhance catalytic activity.[7,8] The relative importance of several possible contributing factors attributable to the pendant carboxyl groups has also not yet been evaluated. Infrared spectroscopic and pH titrimetric studies have established a comparable structural feature in the $L_2Ru^{III}Ru^{IV}$ ion, namely that EDTA is pentacoordinate with one carboxyl group remaining free.[3,5] This ion does not contain coordinated H_2O, however, on the basis of its pH titration behavior.[3] Given these distinct structural features, we felt that a study of the comparative reactivities of the bipyridine- and EDTA-based binuclear ions might provide insight into the catalytic water oxidation mechanisms.

In this report, we present evidence from resonance Raman spectroscopy establishing that $L_2Ru^{III}Ru^{IV}$ is a μ-oxo ion in acidic and neutral solution. We confirm and extend the reported redox behavior of the ion, as deduced from its electrochemical properties,[4] but have been unable to observe dioxygen formation under any of a wide variety of experimental conditions. Instead, we consistently find copious formation of CO_2 accompanied by eventual degradation of the complex ion.

Experimental Procedures

Materials. Aqua(hydrogen ethylenediaminetetraacetato)ruthenium(III) [Ru(Hedta)(OH_2)] was prepared either from $RuCl_3 \cdot 3H_2O$[11] via the intermediacy of Ru(II) blue cluster complexes[12] or by ligand substitution onto the aquapentachlororuthenate(III) [$RuCl_5(OH_2)^{2-}$] dianion.[5] The procedures described in the literature were modified as follows. The immediate product from these reactions was the Ru(Hedta)Cl^- anion, which was isolated as a bright yellow solid of either the sodium[11] or potassium[5] salt. Repeated recrystallization by ethanol addition to 0.01 M trifluoroacetic acid solutions of the complex ion failed to yield the expected Ru(Hedta)(OH_2) compound, but instead the chloro complex was recovered in nearly quantitative yield. Chloride ion was therefore precipitated by adding a 5–10% stoichiometric excess of $AgNO_3$, AgCl removed by centrifugation, and Ru(Hedta)(OH_2) isolated as a tan solid by adding ethanol to the supernatant. The solid product was subsequently recrystallized several times from dilute trifluoroacetic acid/ethanol. Infrared and optical spectral data were very similar to previously reported data;[3,5] in particular, infrared spectra in KBr exhibited strong bands at 1737 and 1656 cm^{-1} attributable to the carbonyl stretching modes of protonated and coordinated carboxyl groups, respectively, and the electronic absorption spectra comprised a broad shoulder at 360 nm and weak maximum at 284 nm superimposed upon a background of increasing absorption at progressively shorter wavelengths.[13] Spot tests with $AgNO_3$ or KCl indicated the absence of detectable Cl^- or Ag^+ ion, respectively, in solutions prepared from the recrystallized solid. No release of Mg^{2+} from Eriochromeschwartz T could be observed spectrophotometrically when the indicator complex was added to a pH 10 ammonia-buffered solution of Ru(edta)$(OH_2)^-$, indicating the absence of unbound EDTA in the preparation; control experiments established that 1% by concentration EDTA could be detected by this method. Considerably higher yields of Ru(Hedta)Cl^- were obtained by the procedure using $K_2Ru(OH_2)Cl_5$ as starting material (~90% vs ~40%). A minor product comprising ~10% of the total yield was isolated from preparations initiated with $RuCl_3 \cdot 3H_2O$ by increasing the ethanol content of the product filtrate. This compound gave an infrared spectrum similar to that of the major product, but differed in having no band at 1727 cm^{-1}. This compound is presumably a ruthenium salt containing hexacoordinated EDTA, similar to complexes isolated from solutions containing $RuCl_3$ and EDTA following other preparative protocols,[14] but was not characterized further. Throughout this study, experimental results for Ru(Hedta)(OH_2) obtained by the two preparative methods were routinely compared without any differences being uncovered.

The $L_2Ru^{III}Ru^{IV}$ ion was usually formed by adding a slight stoichiometric excess of hydrogen peroxide to acidic or neutral solutions of Ru(Hedta)(OH_2). The optical absorption spectrum of this green ion (Figure 1, inset) gave maxima at 632 nm (ϵ = 411 M^{-1} cm^{-1}) and 394 nm (ϵ = 2.00 × 10^4 M^{-1} cm^{-1}); the measured extinction coefficients were intermediate between previously reported values.[3,4] The binuclear ion also formed upon addition of Co^{3+}, Ce^{4+}, ClO_3^-, or MnO_4^- ions in acidic media or by air oxidation in neutral or slightly alkaline solutions. The sodium salt was isolated by adding ethanol to concentrated aqueous

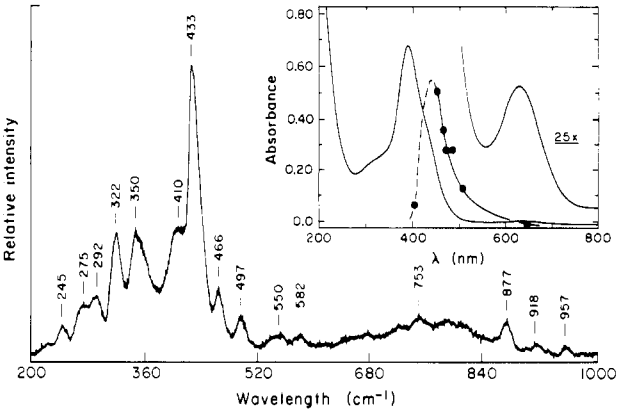

Figure 1. Resonance Raman spectrum of 0.04 M $[Ru(edta)]_2O^{3-}$ ion in 0.3 M acetate buffer, pH 5, with 40-mW excitation at 458 nm; average of 11 scans that was taken by backscattering from a capillary tube containing the frozen sample (90 K). Inset: room-temperature excitation profile scaled to that of 0.3 M SO_4^{2-} ion superimposed upon the electronic absorption spectrum.

solutions, as previously described.[3] The complex was labeled in the bridging position by dissolving Ru(Hedta)(OH_2) in isotopically enriched (85% (Monsanto) or 95% (YEDA) [^{18}O]-H_2O) water that was buffered at pH 4–5 by adding anhydrous sodium acetate. Following incubation at room temperature for 15–30 min, H_2O_2 was added to form the $L_2Ru^{III}Ru^{IV}$ dimer. This period of time is sufficient to equilibrate coordinated H_2O with solvent,[13] but should not allow any significant exchange at the EDTA carboxyl oxygen atoms.[15]

Aqueous solutions of Co^{3+} were prepared by electrolyzing $Co(ClO_4)_2$ in 3 M $HClO_4$ at 1.8 V vs a $Hg/HgSO_4$ reference electrode.[16] Typically, constant-potential electrolysis (CPE) was applied until 30–40% of 30–50 mM Co^{2+} was converted to the Co^{3+} ion. The cobaltic ion content was determined by adding excess $FeSO_4$ and back-titrating with standardized $KMnO_4$. Similarly, reagent solutions of tris(2,2′-bipyridyl)ruthenium(III) ion were prepared by oxidation with PbO_2 and standardized spectrophotometrically. Ceric ion reagent solutions were prepared by dissolving $Ce(NH_4)_2(NO_3)_6$ in $HClO_4$ and filtering to remove precipitated NH_4ClO_4. Other reagents used in this study were the best available grade and were used as received. A conventional reverse-osmosis/ion-exchange system was used to purify water; H_2O that had undergone additional purification by distillation from quartz gave equivalent results.

Methods. Resonance Raman (RR) spectra were recorded on a computer-controlled Jarrel-Ash instrument[17] with excitation from either Spectra-Physics Model 164 argon ion or Spectra-Physics Model 2025 krypton ion lasers. Spectra were usually taken on frozen solutions in capillary tubes at approximately 90 K; spectra of solids were determined by first diluting the sample by grinding with KBr and then placing the material in the trough of a disk to form a ring that could be rotated in the laser beam.[18] In both cases, backscattered photons were collected and analyzed. Fourier transform infrared absorption spectra were taken on a Perkin-Elmer Model 1800 spectrophotometer. Low-temperature electron paramagnetic resonance spectra were obtained with a Varian Model E-109 X-band instrument equipped with an Air Products Model LTR liquid-helium cryostat. The magnetic field was calibrated by using a standard 0.00033% pitch signal, for which g = 2.0028 was assumed. Optical spectra were recorded with a Hewlett-Packard 8452A diode-array spectrophotometer. Gas analyses were made by using either a YSI 4004 polarographic electrode, a Varian Aerograph A90-P3 gas chromatograph containing a 72-cm glass column, 4 mm i.d., packed with 5A molecular sieves, or a VG Analytical 11/250 mass spectrometer operated in the electron-impact mode at 70 eV. For polarographic measurements, the electrode was mounted to sample headspace gases in a reaction cell that could accept reactants and purging gases through septum-fitted openings. For mass spectrometric measurements, reactions were carried out in an evacuable round-bottom flask fitted with a side arm that contained the oxidant. Dissolved gases were first removed by repetitive freeze–pump–thaw cycles on a vacuum line using a dry ice–acetone slurry as coolant. The reaction was then initiated by 180° rotation of the side-arm reservoir, which discharged the oxidant into the main chamber containing solutions of either Ru(Hedta)(OH_2) or the $L_2Ru^{III}Ru^{IV}$ binuclear ion. Evolved gases were collected by condensation under vacuum

(11) Shimizu, K. *Bull. Chem. Soc. Jpn.* **1977**, *50*, 2921.
(12) Rose, D.; Wilkinson, G. *J. Chem. Soc. A* **1970**, 1791.
(13) Matsubara, T.; Creutz, C. *Inorg. Chem.* **1979**, *18*, 1956.
(14) Scherzer, J.; Clapp, L. B. *J. Inorg. Nucl. Chem.* **1968**, *30*, 1107.
(15) Andrade, C.; Jordan, R. B.; Taube, H. *Inorg. Chem.* **1970**, *9*, 711.
(16) Warnqvist, B. *Inorg. Chem.* **1970**, *9*, 682.
(17) Loehr, T. M.; Keyes, W. E.; Pincus, P. A. *Anal. Biochem.* **1979**, *96*, 456.
(18) Sharma, K. D., Ph.D. Dissertation, Oregon Graduate Center, 1988.

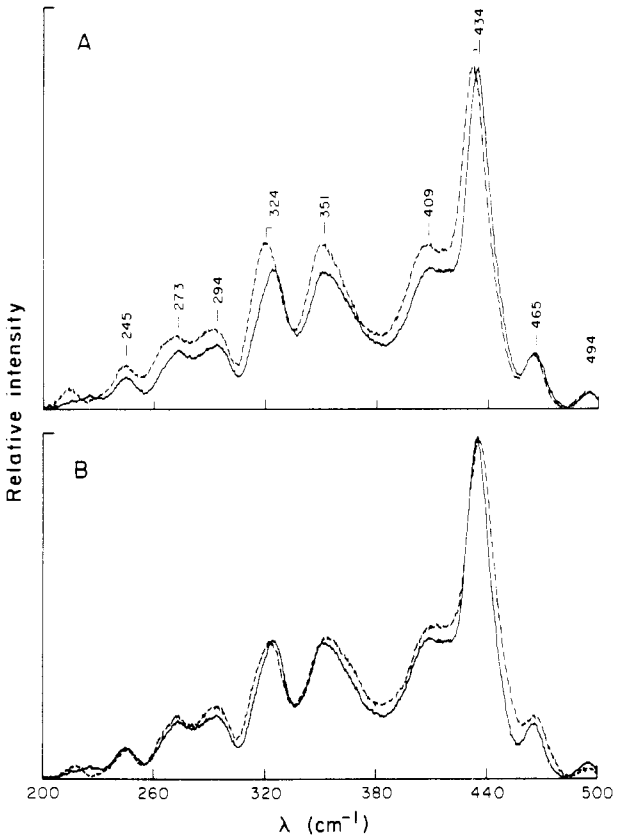

Figure 2. Low-frequency RR spectra of 0.02 M $[Ru(edta)]_2O^{3-}$ ion in 0.24 M acetate, pH 5. Panel A: solid line, ^{16}O bridged; dashed line, ^{18}O bridged. Panel B: solid line, ^{16}O bridged in H_2O; dashed line, ^{16}O bridged in 98% D_2O. Experimental conditions are as in Figure 1, for an average of 10 scans.

in a small tube cooled with liquid nitrogen. This tube was fitted with a microstopcock and ground-glass joint for direct transfer to the mass spectrometer. Spectra were scanned from 20 to 250 amu. Electrochemical preparations and measurements were made by using a PAR Model 273 potentiostat/galvanostat. Cyclic voltammograms were taken by using a glassy-carbon electrode referenced against either $Hg/HgSO_4$ or saturated calomel (SCE) electrodes. Potentials reported herein are referenced against SCE unless otherwise indicated. Spectroelectrochemical measurements were made by using an optically transparent thin-layer electrode equipped with a gold-mesh minigrid;[19] the optical path length of the cell was 0.02 cm.

Results

Vibrational Spectra of $L_2Ru^{III}Ru^{IV}$ Binuclear Ions. FTIR spectra of the (III,IV) dimeric ions taken as their sodium salts in KBr or Nujol exhibited absorption bands attributable to carbonyl stretching modes for protonated (1734 cm^{-1}) and metal-coordinated (1653 cm^{-1}) carboxyl groups, as well as numerous medium to weak bands throughout the 400–600-cm^{-1} region that were similar to but differed slightly in position and/or relative intensities from those found in the spectrum of $Ru(Hedta)(OH_2)$. The largest difference observed in this region was an approximate 2-fold increase in intensity in a band at 876 cm^{-1}, which also shifted to 870 cm^{-1} in the dimer. These spectra are nearly identical with the spectra reported by Baar[5] and also fit the qualitative description given by Ikeda et al.[3] FTIR spectra of the binuclear ions containing ^{16}O or ^{18}O in the ligand bridge were indistinguishable.

The dominant feature of the resonance Raman (RR) spectrum of the dimer in acidic and neutral solution is an intense symmetric band appearing at 433 cm^{-1}; additional medium-intensity bands were found at lower frequencies, but the few bands observed at higher frequencies (to 1100 cm^{-1}) were very weak (Figure 1). Identical spectra were obtained from samples prepared by oxidation of $Ru(Hedta)(OH_2)$ with H_2O_2, ClO_3^-, or O_2. Spectral

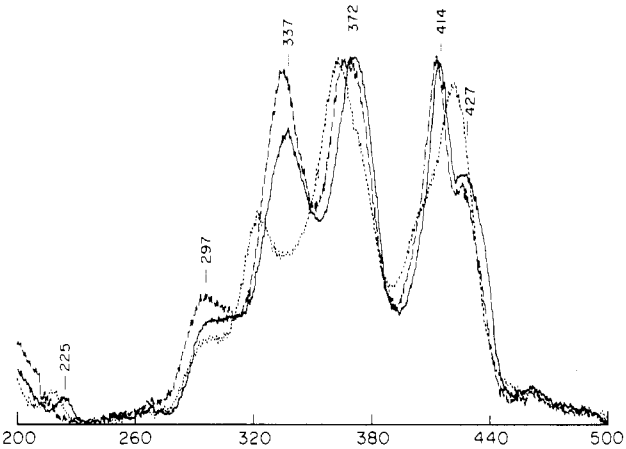

Figure 3. Low-frequency RR spectra of 0.02 M (III,IV)-$[Ru(edta)]_2O$ in 0.01 M NaOH: solid line, ^{16}O bridged in H_2O; dashed line, ^{18}O bridged in 85% $[^{18}O]$-H_2O; dotted line, ^{16}O bridged in 95% D_2O. Experimental conditions are as in Figure 1, for an average of 10 scans.

band shapes were independent of exciting wavelength (456–647 nm), dimer concentration (1.3–40 mM), and medium acidity (pH 2–7). The spectral resolution was considerably improved by freezing the samples in a liquid-N_2 cryostat; at room temperature the medium-intensity modes coalesced and appeared as a broad shoulder on the low-frequency side of the intense peak. The sodium salt diluted in KBr gave a spectrum comparable to the room-temperature solution spectra. In all cases, spectra were unchanged after repetitive scanning, consistent with the absence of interfering photodegradation. However, excitation at higher energies (406 or 413 nm) caused extensive photodecomposition of both solution and solid samples.

Small spectral shifts to lower frequencies occurred in the 433- and 324-cm^{-1} bands when $[^{18}O]$-$Ru(Hedta)(OH_2)$ was used as the dimer precursor (Figure 2). In D_2O, the dimer from $Ru(Hedta)(OH_2)$ containing coordinated water of normal isotopic composition gave barely perceptible (<1 cm^{-1}) shifts of the 433- and 324-cm^{-1} bands to higher and lower frequencies, respectively, as the only spectral perturbations. Above pH 10, the dimer has been shown to undergo optical spectroscopic changes that correlate with the titrimetric uptake of OH^- ion.[4] The RR spectrum of this brown alkaline form exhibited three relatively intense bands from 337 to 414 cm^{-1} whose positions and relative intensities were fairly constant over the alkaline pH region. Each of these bands shifted 2–3 cm^{-1} to lower energies when the dimer was prepared from $Ru(Hedta)(OH_2)$ in isotopically enriched water. Unlike the behavior of the acidic form, these RR bands were sensitive to deuteration, with the 337- and 372-cm^{-1} bands moving to lower energies and the 414-cm^{-1} band apparently shifting to higher energy in D_2O, although the latter effect may be a consequence of changes in relative intensities of the main peak and high-frequency shoulder (Figure 3).

Excitation profiles of the acidic form of the $L_2Ru^{III}Ru^{IV}$ ion were determined by normalizing the scattering intensities of several bands in the room-temperature aqueous spectra to the ν_1 symmetric breathing mode (976 cm^{-1}) of 0.3 M SO_4^{2-} ion, which had been added in the form of its sodium salt. Results for the 433-cm^{-1} band with excitation at various wavelengths from 458 to 647 nm are displayed in the inset to Figure 1. Comparable profiles were obtained for the bands centered at 350 and 272 cm^{-1}. The vibrational modes appear to be coupled to the electronic transition that gives the intense optical band centered at 394 nm. As mentioned above, photobleaching of the sample occurred at shorter excitation wavelengths, precluding quantitative study of scattering intensities over this band.

One-electron oxidation to the corresponding $L_2Ru^{IV}{}_2$ ion has been described[4] (see also below). Addition of a 9-fold excess of Ce^{4+} to $L_2Ru^{III}Ru^{IV}$ in 0.1 M $HClO_4$ (or a 5-fold excess in 0.2 M trifluoroacetic acid) was sufficient to cause quantitative oxidation to the (IV,IV) ion, as was apparent from the optical absorption spectrum. This oxidation state could be maintained

(19) Anderson, C. W.; Halsall, H. B.; Heineman, W. R. *Anal. Biochem.* **1979**, *93*, 366.

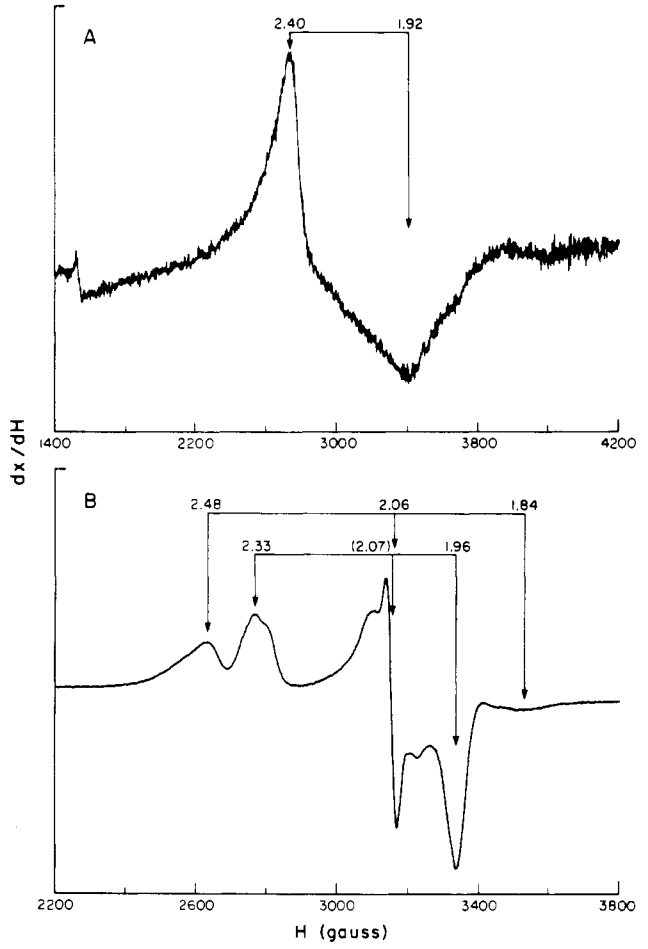

Figure 4. X-Band EPR spectra of (III,IV)-[Ru(Hedta)]$_2$O at 10-mW microwave power and 10-G modulation amplitude: (A) 0.02 M sample in 0.01 trifluoroacetic acid, 5 K; (B) 2 mM sample in 0.01 M NaOH, 20 K. Apparent g values are indicated by the arrows.

indefinitely in frozen solution below 100 K, but reverted to the (III,IV) state under these conditions upon standing at room temperature for 30 min. The low-temperature RR spectrum of the (IV,IV) ion comprised only very broad absorption envelopes centered at 440 and 800 cm^{-1}, from which individual bands could not be resolved. The spectral intensity was maximal with 458–472-nm excitation, and resolution was not improved at other wavelengths. Upon warming, the RR spectrum characteristic of the $L_2Ru^{III}Ru^{IV}$ ion appeared superimposed upon this broad background and grew in intensity with time at the expense of the $L_2Ru^{IV}{}_2$ spectrum. The Ce^{4+} reagent solution did not give detectable Raman bands above 250 cm^{-1}.

Other Physical Properties. (a) Electron Paramagnetic Resonance. In strongly alkaline solution, pH 12–14, the low-temperature EPR spectrum of the $L_2Ru^{III}Ru^{IV}$ ion gave the appearance of a composite of at least two rhombic $S = {}^1/_2$ signals with sets of apparent g values at $g = 2.37$, 2.07, and 1.96 and $g = 2.48$, ~2.07, and 1.84 (Figure 4). The relative intensities of the two sets varied with sample temperature (20–100 K), with the less rhombic signal becoming increasingly predominant at higher temperatures. An aging effect was also evident, with the more asymmetric signal increasing in relative intensity with sample lifetime over a period of several hours when maintained at room temperature. In a less alkaline medium (50 mM glycine, pH 10), the EPR spectrum was even more complex and was dominated by a yet more asymmetric signal with broad bands centered at $g = 2.89$, 2.18, and 1.73 that increased in relative intensity with time. In contrast, the $L_2Ru^{III}Ru^{IV}$ ion in acidic solution gave a much more symmetric signal, which also was considerably weaker (Figure 4).

(b) Electronic Absorption. The $L_2Ru^{III}Ru^{IV}$ ion in alkaline solution exhibited maxima in its optical absorption spectrum at 324 and 412 nm; the 412-nm peak lost intensity over a period of several hours, whereas the intensity of the 324-nm peak was unchanged. The magnitude of the absorbance decrease at 412 nm, which was maximally 50%, was 2-fold greater at pH 12–13 than at pH 11 and was independent of the presence of oxygen. Anaerobic alkaline solutions of the monomeric Ru^{III}(edta) ion underwent no spectral changes over the same time period.

Redox Potentiometry. A typical cyclic voltammogram of Ru(edta)$(OH_2)^-$, taken at pH 7.0, is given in Figure 5. Eight waves are seen over the accessible potential range. Peaks I and III, at −247 and −194 mV, correspond to the reversible one-electron reduction and oxidation of Ru(edta)$(OH_2)^-$ and Ru(edta)$(OH_2)^{2-}$, respectively. Peak II, at −383 mV, was not observed in the initial cathodic scan nor was it observed if the anodic sweep was limited to potentials below 600 mV. In acidic media, another peak that exhibited qualitatively the same behavior was observed at about −70 mV in the cathodic sweep; reversing the scan immediately after passing through this wave revealed the anodic counterpart to this reduction step. These observations are in accord with those of Baar and Anson,[4,5] who have thoroughly studied the electrochemistry of Ru(Hedta)(OH_2) and the $L_2Ru^{III}Ru^{IV}$ ion in this potential region. They assigned the more anodic potential to quasi-reversible one-electron reduction of $L_2Ru^{III}Ru^{IV}$ to $L_2Ru^{III}{}_2$ and the other to irreversible two-electron reduction of the latter ion to Ru(edta)$(OH_2)^{2-}$. The $L_2Ru^{III}{}_2$ ion has also been shown to hydrolyze to Ru(edta)$(OH_2)^-$ on the time scale of the voltammetric sweep.[3,20] Peak IV, at 715 mV in neutral solution, is

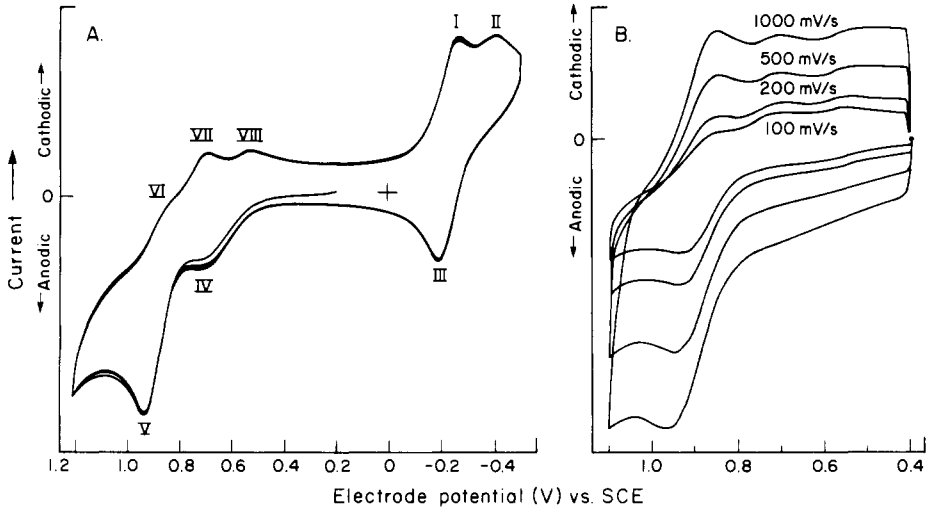

Figure 5. Cyclic voltammograms of 1.8 mM Ru(edta)(OH_2) and 1.3 mM [Ru(edta)]$_2O^{3-}$ ions in 0.1 M phosphate, pH 7.0: (A) monomer, at a scan rate of 100 mV/s, four cycles displayed; (B) dimer, overlay of voltammograms at varying scan rates, but otherwise identical experimental parameters. Glassy carbon, platinum wire, and saturated calomel were used as working, counter, and reference electrodes, respectively.

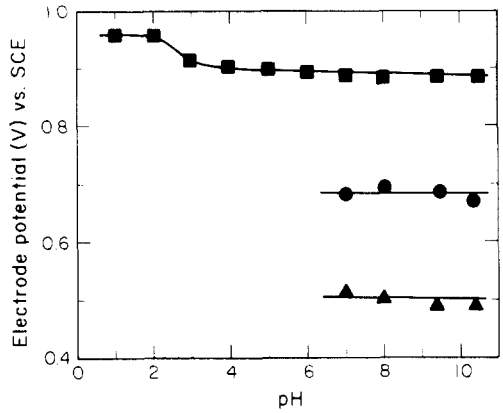

Figure 6. Dependence upon solution acidity of half-cell and peak potentials for waves arising from $[Ru(edta)]_2O^{3-}$ oxidation. Conditions are as in Figure 5. Symbols: (■) E_m(III,IV/IV,IV); (●) peak VII potential; (▲) peak VIII potential.

associated with oxidation of $Ru(edta)(OH_2)^-$ to the $L_2Ru^{III}Ru^{IV}$ ion. It was not observed in the cyclic voltammogram of dimeric $L_2Ru^{III}Ru^{IV}$, provided that the cathodic sweep was not carried beyond about −100 mV, the point at which reduction gives rise to formation of monomeric complex ions. Furthermore, CPE of monomer solutions at 800 mV yielded the green $L_2Ru^{III}Ru^{IV}$ ion. Peak V, at 920 mV, has been shown by Baar and Anson to be the one-electron oxidation of $L_2Ru^{III}Ru^{IV}$ to $L_2Ru^{IV}{}_2$.[4] We have confirmed their spectrophotometric identification of this ion by CPE in a thin-layer cell. Specifically, electrolysis at 1.0 V vs SCE caused the expected maximum to shift from 394 to 428 nm, with accompanying disappearance of the 624-nm band. We assign peak VI, at 860 mV, to the coupled quasi-reversible $L_2Ru^{IV}{}_2 \rightarrow L_2Ru^{III}Ru^{IV}$ step from the magnitude of its reduction potential. Peaks VII and VIII, at ~690 mV and ~500 mV, respectively, are also associated with oxidation to the (IV,IV) level because they are not observed if the anodic sweep is reversed at potentials below 800 mV. Furthermore, the amplitudes of peaks VII and VIII increased relative to peak VI with decreasing scan rate (Figure 5B), suggesting that they represent species derived from the $L_2Ru^{IV}{}_2$ ion. Reversing the sweep immediately after passing cathodically through peaks VII or VIII showed the presence of coupled anodic waves for each step at ~750 and ~560 mV, respectively (not shown), although these waves nearly disappeared within the time required for complete cycling. Below pH 6.5, peak VI was the predominant cathodic wave among this set. The chemical nature of species that might correspond to peaks VII and VIII will be discussed in succeeding sections. The cyclic voltammograms of the $L_2Ru^{III}Ru^{IV}$ ion differed from those of $Ru(edta)(OH_2)^-$ in the following respects: (i) no oxidation waves were observed below 900 mV in the first cycle of scans initiated in the anodic direction, but subsequent scans exhibited waves assignable to the oxidizing counterparts of peaks VII and VIII if the cathodic sweep was reversed above −100 mV and to peak IV if the scan range was extended to −500 mV; (ii) peak I was absent from the first cycle of scans initiated in the cathodic direction, but was prominent in subsequent cycles. These results are consistent with the reaction scheme and peak assignments deduced form the electrochemical behavior of the $Ru(edta)(OH_2)^-$ ion[4] (see above). The pH dependence of half-cell and peak potentials for waves arising from $L_2Ru^{III}Ru^{IV}$ ion oxidation are given in Figure 6.

Decomposition of the $L_2Ru^{IV}{}_2$ Ion. Addition of excess strong oxidant, i.e., with $E_0' > 1.0$ V vs SCE, caused immediate conversion to the $L_2Ru^{IV}{}_2$ ion, which was identified by its characteristic absorption band at 428 nm.[4] Chemical oxidants used in this study included Co^{3+}, Ce^{4+}, and MnO_4^- ions in strongly acidic media and $Ru(bpy)_3^{3+}$ in weakly acidic media (pH 4–5); oxidation was also accomplished electrochemically by CPE at 0.6 V vs Hg/

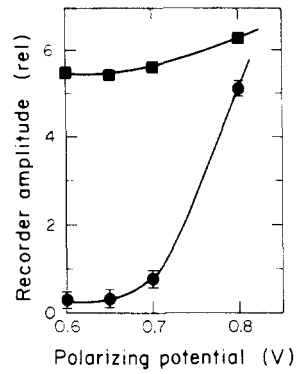

Figure 7. Response of the Clark electrode to air (■) and CO_2 (●) at various potentials relative to Ag/AgCl. 1 mL of gas was injected into 5 mL of headspace over 4 mL of H_2O to give the following effective concentrations: $[CO_2] = 8$ mM, or $[O_2] = 1.6$ mM. Data were averages of three measurements; analogous behavior was obtained when the gases were injected into a dry cell or directly into the liquid, but injection of 1 mL of argon gave no response.

$HgSO_4$ over the entire acid–alkaline range. As previously reported, the $L_2Ru^{IV}{}_2$ ion was unstable under all conditions, and over a period of minutes to hours its spectrum reverted to the spectrum of the $L_2Ru^{III}Ru^{IV}$ ion. Some bleaching of the solution occurred, however, which was particularly evident at longer electrolysis times or for large concentration excesses of oxidant. Semiquantitative estimates of the stoichiometry of bleaching were made by sequentially adding 5-fold concentration excesses of Ce^{4+} ion, with sufficient time being given between additions for equilibration of the system. After the first addition, the final spectrum gave an absorbance at 394 nm that was identical with the value expected for simple dilution of the $L_2Ru^{III}Ru^{IV}$ ion, but deviations from quantitative recovery appeared and became progressively greater with subsequent additions, so that by the fourth cycle 22% of the complex absorption had been lost. At this point, the apparent redox stoichiometry corresponded to 91 Ce^{4+} ions reduced/dimer bleached.

The gaseous products formed upon reduction of the $L_2Ru^{IV}{}_2$ ion were analyzed by several techniques. Adding any of the oxidants used in acidic media gave an immediate response from a Clark polarographic electrode located in the headspace of the reaction cell when the electrode was poised at −0.8 V vs its internal Ag/AgCl reference electrode. The reducible gas accumulated approximately in parallel with solution optical changes, and its evolution ceased when the $L_2Ru^{IV}{}_2$ ion was depleted. No response was observed when the $L_2Ru^{III}Ru^{IV}$ ion was oxidized chemically or electrochemically in alkaline solution or under any conditions when the Clark electrode was poised at −0.6 V vs its internal reference. However, acidifying alkaline solutions following oxidation–reduction cycling, i.e., after the redox processes were completed, gave immediate response from the electrode if poised at −0.8 V vs Ag/AgCl. Control experiments such as given in Figure 7 established that the electrode responded to both CO_2 and O_2 when poised at −0.8 V, but only to O_2 at −0.6 V. No O_2 could be detected beyond that attributable to contamination with air during injection, i.e., appearing in a N_2/O_2 ratio of 4.0, when headspace gases from spent reactions were analyzed with a gas chromatograph. These results implicate CO_2, rather than O_2, as the gas formed during $L_2Ru^{IV}{}_2$ ion reduction. This suggestion was confirmed for the acidic reactions with strong oxidants by collection and mass spectrometric analysis of condensable product gases (Figure 8). The small amount of O_2 present in the mass spectrum is attributable from the N_2/O_2 ratio to background air in the instrument.

The amount of CO_2 formed by $L_2Ru^{III}Ru^{IV}$ reaction with various oxidants and by reaction at a platinum anode under diverse experimental conditions was determined with the Clark electrode by using calibration curves constructed by injecting known amounts of CO_2 under equivalent experimental conditions. The results are summarized in Table I. Evidence for O_2 formation was sought under all experimental conditions for which data are

(20) Ni, C.-L.; Anson, F. C.; Osteryoung, J. G. *J. Electroanal. Chem. Interfacial Electrochem.* **1986**, *202*, 101.

Table I. CO_2 Yields from Reactions of $[Ru(Hedta)]_2O$ with Strong Oxidants[a]

oxidant	μequiv of oxidant	μmol of dimer	pH[b]	μmol of CO_2	oxidant/CO_2
Ce^{4+}	8–25	1.0	1.0	4–10	2.1–2.5[c]
	50	1.0	1.0	10	5.0
MnO_4^-	45–80	2.0	1.0	16–21	2.8–3.8[c]
Co^{3+}	16–51	0.3–1.8	0.4 ($HClO_4$)	7–26	2.0–3.2
$Ru(bpy)_3^{3+}$	12	1.2	4.4 (1 M acetate)	4.5	2.7
Pt anode[d]	5.5–46	5.0	7–11 (0.1 M PO_4)[e]	3–22	2–9[f]

[a] Excepting CPE experiments, reaction was initiated by anaerobic addition of oxidant to the dimer in 4 mL of total volume at ambient temperature. [b] Trifluoroacetic acid, unless otherwise indicated. [c] Ratios increased monotonically with increasing oxidant concentration. [d] Poised at 0.45 V vs $Hg/HgSO_4$ (0.85 V vs SCE). [e] At pH 13, copious evolution of CO_2 occurred, but solvent oxidation may have caused a large overestimate of current passed. [f] Ratio increased with decreasing pH.

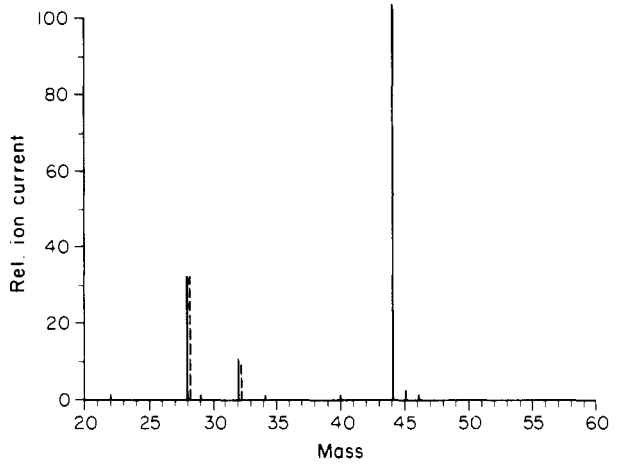

Figure 8. Mass spectra of headspace gases following MnO_4^- oxidation of (III,IV)-$[Ru(Hedta)]_2O$. Conditions: $[MnO_4^-]$ = 13 mM; $[Ru_2O]$ = 0.5 mM, pH 1 ($HClO_4$). The dashed line gives relative intensities of background scaled to N_2.

reported by using the Clark electrode poised at −0.6 V. A positive response beyond the small deflection attributable to CO_2 was never observed at this potential, however.

Discussion

Nature of the Ligand Bridge. Recent studies[3-5] have eliminated from consideration many of the diverse types of ligand bridges proposed earlier for the $L_2Ru^{III}Ru^{IV}$ ion; these data are consistent only with formulations of μ-oxo- or dihydroxy-bridged structures. Our resonance Raman results establish that the bridge is a μ-oxo ion. Three normal-coordinate vibrational motions exist for this type of bridge, comprising asymmetric, ν_{as}(M–O–M), and symmetric, ν_s(M–O–M), stretching modes and a bending, δ(M–O–M), mode. For a bent M–O–M unit, all three modes are Raman active, but ν_s is expected to be much more intense than the others. The frequencies of ν_s and ν_{as} modes are, in principle, highly variable and depend strongly upon the M–O–M angle, but for nearly linear bridges, ν_s = 300–500 cm^{-1} and ν_{as} = 750–950 cm^{-1} are reasonable theoretical estimates.[21] Experimental results from a variety of μ-oxo-bridged systems, including biological dimeric ions, confirm these expectations.[22] To fit these data, the δ(M–O–M) mode is calculated to lie below 200 cm^{-1}; however, a vibrational band that is sensitive to isotopic substitution in the bridge is often observed at frequencies close to 300 cm^{-1}. For this reason, it has been suggested[22] that the δ(M–O–M) mode is coupled to other ligand vibrations in the molecule, most prominently the stretching motion of the ligand atom trans to the μ-oxo bridge.

The $L_2Ru^{III}Ru^{IV}$ ion in acidic to weakly alkaline media displays two RR bands, at 434 and 324 cm^{-1} (Figure 2), that are sensitive to ^{18}O substitution in the bridge; their positions and relative intensities are analogous to results from model studies, which support their assignment to the ν_s(Ru–O–Ru) and ligand-mixed δ(Ru–O–Ru) modes, respectively. The ν_{as}(Ru–O–Ru) mode was not observed. The small magnitudes of the isotopic shifts, $\Delta\epsilon$ = 1–2 cm^{-1}, and the virtual absence of a deuterium isotope effect (Figure 2) establish that the 434- and 324-cm^{-1} bands are not attributable to metal–aquo ligand stretching motions and that the bridging oxo atom is deprotonated. (The barely detectable shift to *higher* frequencies of ν_s in D_2O may be attributable to hydrogen bonding to solvent; very similar effects observed in metalloproteins containing binuclear Fe–O–Fe centers have been attributed to internal hydrogen bonding to the μ-oxo atom.[22]) The cumulative data from this and earlier studies are therefore consistent only with a simple μ-oxo-monobridged structure. From the magnitude of the ^{18}O-induced shift in ν_s, a Ru–O–Ru angle of 165° is estimated[21] for the $L_2Ru^{III}Ru^{IV}$ μ-oxo dimer.

A peroxy-bridged dimeric ion has been proposed[2] to form upon air oxidation of $Ru(edta)(OH_2)^-$; this assignment was based upon observation of a new band appearing at 890 cm^{-1} in the absorption infrared spectrum, which was attributed to the peroxy symmetric stretching motion. We did not observe this band in dimeric ions prepared with various oxidants, but instead found that a weak band at 870 cm^{-1} in $Ru(edta)(OH_2)^-$ intensified upon oxidative dimerization. None of the dimer bands, measured between 400 and 4000 cm^{-1}, shifted when ^{18}O was substituted in the bridging position. Furthermore, air-oxidized $Ru(edta)(OH_2)^-$ gave RR spectra of the frozen solution and the isolated solid that were identical with those for the μ-oxo dimer prepared by other means.

Other Ligands. None of the bands in the RR spectrum of the $L_2Ru^{III}Ru^{IV}$ μ-oxo ion are attributable to coordinated water. Differences in zero-point vibrational energies upon substitution of ^2H and ^{18}O would lower energies of simple Ru–O stretching motions by 9–17 cm^{-1}, respectively, which is far greater than any observed isotope-induced shift (Figure 2). We were also unable to identify by this method the Ru–O stretching vibration of H_2O in *cis,cis*-$[Ru(bpy)_2(OH_2)]_2O^{4+}$,[29] a μ-oxo ion whose structure has been established by X-ray crystallography.[6] One therefore cannot conclude from these measurements that the $L_2Ru^{III}Ru^{IV}$ μ-oxo ion does not coordinate solvent. However, pH measurements have indicated the absence of titratable protons in the region of pH 2–10 for the dimer,[3] whereas $Ru(edta)(OH_2)^-$ exhibits loss of a single proton with a pK_a = 7.6.[13] On the basis of these observations, the dimeric ion can be identified as $[Ru(Hedta)]_2O^-$, with the ligand environment of each ruthenium presumably including pentacoordinate EDTA and the μ-oxo atom.

Apart from a small increase above pH 2 attributable to protonation of the pendant carboxylate groups,[13] the half-wave potential for one-electron oxidation is pH-independent to pH 10–11 (Figure 6). This result indicates that the initially formed $L_2Ru^{IV}{}_2$ μ-oxo ion also possesses no bound H_2O, since coordination would undoubtedly occur with release of protons in this pH domain, e.g., as in

$$2H_2O + [Ru(edta)]_2O^{2-} \rightarrow [Ru(edta)(OH)]_2O^{4-} + 2H^+$$

Primary-sphere solvation should therefore give rise to half-wave reduction potentials that increase with solution pH, contrary to the observed behavior.

The additional reduction waves appearing at 712 and 539 mV in the cyclic voltammograms above pH 6 have several possible origins. They were attributed by Baar to electrode adsorption

(21) Wing, R. M.; Callahan, K. P. *Inorg. Chem.* **1969**, *8*, 871.
(22) Loehr, T. M.; Shiemke, A. K. In *Biological Applications of Raman Spectroscopy*; Spiro, T. G., Ed.; Wiley: New York, 1988, Vol. 3; Chapter 10.

phenomena,[5] but have anodic half-waves that suggest quasi-reversible processes. Alternatively, they might represent species that have undergone aquation at one or more EDTA ligation sites. This notion is consistent with their lower reduction potentials since hydroxo ligands formed by deprotonation should preferentially stabilize the higher oxidation state.[10] A third possibility is that these species are products of $[Ru(edta)]_2O^{2-}$ ion decomposition since it is apparent that the complex in the (IV,IV) oxidation state is unstable with respect to CO_2 evolution (Table I). This latter circumstance does not exclude aquation since loss of EDTA binding sites will ultimately accompany degradation of the ligand. The short lifetimes of these intermediary ions, which are less than the voltammetric sweep times, compromise attempts to identify them.

In alkaline solution, pH >11, the RR spectrum of the (III,IV) μ-oxo ion becomes more complex and is dominated by three bands in the low-frequency region, each of which undergoes small shifts to lower energies when $[^{18}O]$-H_2O is coordinated in the precursor $Ru(edta)(OH_2)^-$ ion (Figure 3). If ligation were restricted solely to EDTA and the μ-oxo atom, this result would imply the existence of at least two discrete species. However, more dramatic frequency shifts, both upfield and downfield, are found in D_2O (Figure 3). The magnitudes of the shifts in the 372- and 337-cm^{-1} bands, $\Delta\epsilon$ = 10–14 cm^{-1}, are sufficiently large that these bands might be assigned to Ru–O stretching motions of coordinated hydroxide ion, were it not for the much smaller shifts accompanying substitution of the heavier oxygen isotope. (Since the isotopically substituted dimers were prepared in $H_2{}^{18}O$-enriched solvent, hydroxide substitution upon alkalinization would lead to incorporation of ^{18}O in these positions as well.) On the basis of spectroscopic and titrimetric data indicating reversible uptake of one OH^- per dimer, Baar and Anson have proposed[4] formation of a mixed-dibridged structure comprising one oxo and one hydroxo ligand which is governed by an equilibrium pK_a of 10.3. It is not apparent that the vibrational properties of this ion can solve the dilemma posed by larger isotope shifts arising from deuterium than from ^{18}O substitution. Several additional observations suggest that the structural properties of the dimeric ions in alkaline solution are more complicated. These include the differential temperature dependence for the rhombic EPR signals of the alkaline ions and the temporal changes in both their EPR and optical properties described in the Results. It should also be noted that our alkaline EPR spectra are very similar to spectra previously reported by Baar,[5] although major differences exist in our spectra of the μ-oxo dimer under more acidic conditions. From these data, it appears that multiple dimeric species can exist in alkaline solution, and the prospect exists that some of these might be formed by solvent substitution at EDTA-binding sites.

Catalysis vs Ligand Decomposition. The one-electron-reduction potential of the $[Ru(edta)]_2O^{2-}$ ion, approximated by E_m = 0.9 V (Figure 6), is clearly insufficient to drive one-electron oxidation of water, for which $E_7°'(OH/H_2O)$ = 2.16 V, relative to SCE.[23] The potentials for two- and three-electron reduction to $[Ru(edta)]_2O^{4-}$ and $[Ru(edta)]_2O^{5-}$, respectively, can be estimated from the midpoint potentials[24] for reduction of the $Ru^{IV}{}_2$, $Ru^{III}Ru^{IV}$, and $Ru^{III}{}_2$ dimers to be $E_7°'(IV,IV/III,III)$ = 0.38 V and $E_7°'(IV,IV/III,II) \sim 0.14$ V. The latter value is relatively uncertain because the $Ru^{III}{}_2$ ion is highly unstable and correspondence of its reduction wave to a one-electron process has not been firmly established.[25] Nonetheless, the formal potentials[23] for two- and three-electron reduction of H_2O_2 and O_2^- are $E_7°'(H_2O_2/H_2O)$ = 1.08 V and $E_7°'(O_2^-/H_2O)$ = 0.96 V, again indicating energetically highly unfavorable water oxidation pathways. The driving force for four-electron oxidation cannot be calculated because the $Ru^{III}Ru^{II}/Ru^{II}{}_2$ potential is unknown, but even with the $Ru^{III}{}_2/Ru^{III}Ru^{II}$ potential taken as an upper limit, it is still unfavorable by 0.5 V. The stoichiometric equations for water oxidation by the dimer generally involve proton release; consequently, the energetics for these reactions become more favorable in alkaline solution. Nonetheless, even at pH 12, the thermodynamic barrier remains greater than 0.4 V for each of these reactions. It is clear, then, that the $[Ru(edta)]_2O^{2-}$ ion is thermodynamically incapable of oxidizing H_2O.

Baar and Anson have suggested that O_2 formation might occur by disproportionation to give in low yield a more highly oxidized and reactive complex.[4] One plausible mechanism for rendering accessible higher oxidation states of the dimer is partial aquation of the initially formed $Ru^{IV}{}_2$ ion.[6,10] Aquation might also introduce new catalytic pathways by allowing coordinative stabilization of intermediary species formed upon oxidation of ligated water. These possibilities cannot be assessed because relevant thermodynamic data are unavailable. From our perspective, this discussion is hypothetical since we have been unable to detect O_2 formation, even in highly alkaline media where both OH^- ligation and the energetics of water oxidation are favored. In fact, in CPE experiments, CO_2 evolution rates were greater under more alkaline conditions.

EDTA is susceptible to oxidation by strong oxidants,[26] and coordination complexes containing certain redox metal ions undergo photodegradation upon illumination of their CTTM bands to yield CO_2.[27,28] Under the experimental conditions of this study, rapid evolution of CO_2 occurs upon addition of the chemical oxidants to EDTA-containing solutions. The reaction stoichiometry for complete oxidation of EDTA can be written as

$$34Ce^{4+} + 12H_2O + C_{10}H_{16}N_2O_8 \rightarrow 34Ce^{3+} + 10CO_2 + 2NH_4^+ + 32H^+$$

Therefore, up to 68 Ce^{4+} ions/dimer may be required for oxidative bleaching of the complex, assuming no change in the metal oxidation state. The titrimetric behavior described in the Results suggests more complicated behavior, however. Specifically, additions of severalfold excess Ce^{4+} ion initially gave imperceptible net spectral changes following exhaustion of the oxidant, although CO_2 was evolved (as measured with the Clark electrode). Thus, the immediate reaction product gave an absorption spectrum very similar to the reactant $[Ru(edta)]_2O^{3-}$ ion. This behavior suggests that the initial reaction involves preferential reaction of the pendant carboxyl group. By analogy with photodecomposition of metal EDTA complexes, the immediate reaction products would include CO_2 and either ligated *N*-methylethylenediaminetriacetate[28] or ethylenediaminetriacetate.[27] Because in this instance the initial product is still probably pentacoordinated through an N_2O_3 ligand set, its absorption spectrum should be very similar to that of the reactant.[28] Subsequent oxidation may lead to loss of the ligand, followed by its preferential reaction with the remaining oxidant. This behavior would account for both the absence of spectroscopically detectable intermediates and the decreasing Ce^{4+}/dimer bleaching stoichiometry that accompanies progressive oxidation of the complex. The theoretical limit for complete EDTA oxidation, i.e., oxidizing equivalents/dimer = 68, is probably not achievable because other fragmentary oxidation products that are resistant to further oxidation, e.g., formic acid,[26,27] may form. In our experiments, the oxidant was always the limiting reagent. Under these conditions, the oxidant/CO_2 ratio (Table I) was generally less than the value for complete EDTA oxidation (3.4), which also supports the idea that CO_2 is first formed from the more highly oxidized, i.e., carboxylate, ligand carbon atoms.

To summarize, the $[Ru(edta)]_2O^{3-}$ ion appears incapable on thermodynamic grounds of catalyzing water oxidation and other potentially catalytic complexes that might be derived from it are

(23) Koppenol, W. H.; Butler, J. *Adv. Free Radical Biol. Med.* **1985**, *1*, 91.
(24) One-electron midpoint reduction potentials at pH 7 are taken to be as follows: for $Ru^{IV}{}_2$, E_m = 0.89 V;[4] for $Ru^{III}Ru^{IV}$, E_m = –0.13 V;[4,5] for $Ru^{III}{}_2$, $E_m \simeq$ –0.33 V.[5]
(25) An ECE mechanism, comprising one-electron reduction of $Ru^{III}{}_2$ followed by rapid hydrolysis to monomers and subsequent reduction of the Ru(III) monomer, has been proposed, based upon pulse polarographic and rotating ring–disk electrode results.[5]
(26) See, for example, Skoog, D. A.; West, D. M. *Fundamentals of Analytical Chemistry*; Holt, Rinehart, and Winston: New York, 1963; pp 448, 454–456.
(27) Carey, J. H.; Langford, C. H. *Can. J. Chem.* **1973**, *51*, 3665.
(28) Natarajan, P.; Endicott, J. F. *J. Phys. Chem.* **1973**, *77*, 2049.
(29) Hurst, J. K. Unpublished observations.

too unstable with respect to ligand oxidation to function effectively in this capacity.

Acknowledgment. We have benefited from discussions with Arthur J. Frank and Roger Palmans (SERI, Golden, CO) and Francois P. Rotzinger (EPFL, Lausanne, Switzerland). Funding for this research was provided by the Office of Basic Energy Sciences, U.S. Department of Energy, under Grant DE-AC-06-83ER-13111. We are grateful to them for their interest and support.

Contribution from the Department of Chemistry,
The University of North Carolina at Charlotte, Charlotte, North Carolina 28223

Multimetallic Ruthenium(II) Complexes Based on Biimidazole and Bibenzimidazole: Effect of Dianionic Bridging Ligands on Redox and Spectral Properties

D. Paul Rillema,* Ram Sahai, Philomina Matthews, A. Kirk Edwards, Randy J. Shaver, and Larry Morgan

Received May 1, 1989

The preparation and properties of ruthenium(II) complexes containing the ligands 2,2′-biimidazole ($BiImH_2$), 2,2′-bibenzimidazole ($BiBzImH_2$), and 2,2′-bipyridine (bpy) are reported. The complexes described are $[(Ru(bpy)_2)_2BiIm]^{2+}$ and the series $[Ru(bpy)_n(BiImH_2)_{3-n}]^{2+}$, $[Ru(bpy)_n(BiBzImH_2)_{3-n}]^{2+}$, and $[Ru(bpy)_n(BiBzImRu(bpy)_2)_{3-n}]^{2+}$, $n = 0$–2. The redox potential for the first $Ru^{3+/2+}$ couple shifted negatively from 1.26 to −0.26 V vs SSCE as bpy ligands were replaced by $BiImH_2$, $BiBzImH_2$, and "$BiBzImRu(bpy)_2$" ligands. The $BiBzImRu(bpy)_2$ units shifted the redox potential a factor of 3 greater than that for $BiBzImH_2$, which was attributed to greater electrostatic interaction of the dinegatively charged bridging ligands following deprotonation. The magnitude of the shift was such that the tetrametallic species was isolated as the $[Ru^{III}(BiBzImRu^{II}(bpy)_2)_3)]^{3+}$ cation. Reductions were found in the −1.5- to −1.6-V range for complexes containing bipyridine ligands, but none were observed out to −2.0 V for $[Ru(BiImH_2)_3]^{2+}$ or $[Ru(BiBzImH_2)_3]^{2+}$. The complexes absorbed energy in the visible and UV regions of the spectrum and emitted radiation, with the exception of the tetrametallic species, in the 600–800-nm region. The emission was weak, $\phi_r = 10^{-3}$–10^{-4}; the excited-state lifetimes ranged from 25 to 161 ns. Estimates of the excited-state redox potentials revealed that the excited-state species were powerful reductants, $E_{1/2}(Ru^{3+/2+*}) \sim -0.8$ V, but were weak oxidants, $E_{1/2}(Ru^{2+*/+}) \sim 0.2$ V. The $[Ru^{III}(BiBzImRu^{II}(bpy)_2)_3]^{3+}$ cation absorbed in the near-infrared region at 12.2×10^3 cm^{-1} in acetonitrile, but the absorption disappeared upon reduction to $[Ru^{II}(BiBzImRu^{II}(bpy)_2)_3]^{2+}$. The position of the absorption manifold maximum varied linearly with the static and optical dielectric constant of the solvent. The width of the absorption band was comparable to that of $[Ru^{III}(bpy)_2BiBzImH_2]^{3+}$, but its intensity was greater. The band at 12.2×10^3 cm^{-1} was attributed to overlapping LMCT and metal to metal charge transfer.

Introduction

Studies in our laboratories have centered on the design of multimetallic complexes based on bidentate bridging ligands with the ultimate goal of effecting multiple-electron-transfer events from excited-state species. Our efforts have resulted in the isolation of ruthenium/ruthenium,[1,2] ruthenium/platinum,[3-5] and ruthenium/rhenium[6] complexes. We have, for example, isolated the $[Ru(bpqRu(bpy)_2)_3]^{8+}$, $[Ru(bpqPtCl_2)_3]^{2+}$, and $[Ru(bpmRe(CO)_3Cl)_3]^{2+}$ cations as PF_6^- salts, where bpq is 2,3-bis(2-pyridyl)quinoxaline, bpm is 2,2′-bipyrimidine, and bpy is 2,2′-bipyridine. The multimetallic complexes were formed by addition of the appropriate precursor to the remote nitrogen donors on the ligands of the parent $[Ru(bpq)_3]^{2+}$ and $[Ru(bpm)_3]^{2+}$ complexes. The presence of more than one metal with these bridging ligands shifts the luminesce to the red side of the spectrum approximately 100 nm and decreases the luminescence intensity by at least 1 order of magnitude.[7] However, complexes formed from bridging ligands with a saturated alkyl linkage retained their luminescence integrity. The $[(bpy)_2Ru(Mebpy\text{-}Mebpy)PtCl_2]^{2+}$ complex, for example, where Mebpy-Mebpy is 1,2-bis(4′-methyl-2,2′-bipyridiyl-4-yl)ethane, was nearly as emissive[4] as $[(bpy)_2Ru(Mebpy\text{-}Mebpy)]^{2+}$.

In this paper, we report complexes based on a different type of bridging ligand. Biimidazole and bibenzimidazole shown in Figure 1 were used to effect bridging from one ruthenium(II) center to another and enabled us to prepare $[(Ru(bpy)_2)_2BiIm]^{2+}$ and the series $[Ru(bpy)_n(BiImH_2)_{3-n}]^{2+}$, $[Ru(bpy)_n(BiBzImH_2)_{3-n}]^{2+}$, and $[Ru(bpy)_n(BiBzImRu(bpy)_2)_{3-n}]^{2+}$, $n = 0$–2. There was reason to believe that complexes of this type could be formed with these ligands. Bimetallic complexes based on these ligands have been reported by several authors. Some examples are $[Rh_2(COD)_2(BiIm)]$,[8] $[Ir_4(CO)_8(BiIm)_2]$,[9] $[Cu_2(dien)_2(BiBzIm)](BPh_4)_2$,[10] $(NBu_4)_2[Pd_2(C_6F_5)_4(BiBzIm)]$,[11] $[(Mn(CO)_3PPh_3)_2(BiIm)]$,[12] $[(W(\eta\text{-}C_5H_5)_2)_2(BiIm)](PF_6)_2$,[13] and $[((bpy)_2Ru)_2BiBzIm](ClO_4)_2$.[14]

The biimidazole and bibenzimidazole ligands require deprotonation in order to form bidentate chelated complexes. In a related study Meyer and co-workers[15] studied the properties of

(1) Rillema, D. P.; Callahan, R. W.; Mack, K. B. *Inorg. Chem.* **1983**, *22*, 1617.
(2) Sahai, R.; Morgan, L.; Rillema, D. P. *Inorg. Chem.* **1988**, *27*, 3495.
(3) Sahai, R.; Rillema, D. P. *Inorg. Chim. Acta* **1986**, *118*, L32.
(4) Baucom, D. A.; Rillema, D. P. *Inorg. Chem.* **1986**, *25*, 3843.
(5) Sahai, R.; Rillema, D. P. *J. Chem. Soc., Chem. Commun.* **1986**, 1133.
(6) Sahai, R.; Rillema, D. P.; Shaver, R.; Van Wallendael, S.; Jackman, D. C.; Boldaji, M. *Inorg. Chem.* **1989**, *28*, 1022.
(7) Fuchs, Y.; Lofters, S.; Dieter, T.; Shi, W.; Morgan, R.; Strekas, T. C.; Gafney, H. D.; Baker, A. D. *J. Am. Chem. Soc.* **1987**, *109*, 2691.
(8) Kaiser, S. W.; Saillant, R. B.; Butler, W. M.; Rasmussen, P. G. *Inorg. Chem.* **1976**, *15*, 2681.
(9) Kaiser, S. W.; Saillant, R. B.; Butler, W. M.; Rasmussen, P. G. *Inorg. Chem.* **1976**, *15*, 2688.
(10) Huddad, M. S.; Hendrickson, D. H. *Inorg. Chem.* **1978**, *17*, 2622.
(11) Uson, R.; Gimeno, J.; Fornie, S.; Martinez, F. *Inorg. Chim. Acta* **1981**, *50*, 173.
(12) Uson, R.; Gimeno, J. *J. Organomet. Chem.* **1981**, *220*, 173.
(13) Calchorda, M. J.; Dias, A. R. *J. Organomet. Chem.* **1980**, *197*, 291.
(14) Haga, M.-A. *Inorg. Chim. Acta* **1980**, *45*, L183.
(15) Sullivan, B. P.; Salmon, D. J.; Meyer, T. J.; Peedin, J. *Inorg. Chem.* **1979**, *18*, 3369.

0020-1669/90/1329-0167$02.50/0